Arch Appl Mech (2006)
DOI 10.1007/s00419-005-0418-1

ORIGINAL

Chen Ying · Shi Zhifei

Double-layered piezo-thermoelastic hollow cylinder under some coupled loadings

Received: 18 November 2004 / Accepted: 18 June 2005 / Published online: 15 February 2006

Abstract In the present paper, a long thick-walled piezo-thermoelastic hollow cylinder with double layers is studied. The effects of temperature on the performance of the cylinder are obtained. Based on the theory of elasticity, the exact solutions of the cylinder under some coupled loadings are found. In the present paper, differences of a piezoelectric parameter between the two layers is taken into account. For comparison, numerical results have been carried out for both double-layered and graded cylinders. At the end of the present paper some discussions are addressed.

Keywords Piezo-thermoelastic material · Thick-walled hollow cylinder · Elastic analysis · FGM · Transducer · Sensors and actuators

1 Introduction

Since the Curie brothers discovered the piezoelectric effect in 1880, piezoelectric materials and structures have received considerable attention because of their potential for designing adaptive structures with control capabilities. Piezoelectric symmetric structures always play an important role in this field. To date, a large number of investigations have been completed, on a variety of these structures, such as studies on the static behaviors of an elastic cylinder [1] and piezoelectric tube [2,3], the dynamic properties of a hollow piezoelectric sphere/cylinder [4,5] and a piezo-thermoelastic cylindrical panel [6], and so on.

In recent years, it has been realized that temperature loading is sometimes so high that it is the predominant reason for failure of smart structures. Therefore the mechanical response of structures excited by thermal loading is of increasing interest in engineering research and a large number of investigations have been made on these subjects. For example, theoretical analysis of the control of displacement was developed for a composite rectangular plate constructed from an isotropic elastic layer and a piezoelectric layer due to nonuniform heat supply [7], and the thermal stress distribution in a particle-reinforced functionally gradient material (FGM) [8] or piezo-thermoelastic plate [9,10] was obtained. On the other hand, the investigation of the effects of temperature on piezoelectric sensors found that even moderate fluctuations of temperature within 200°C could significantly change the voltage reading from the sensors [11]. In this investigation the geometric nonlinearity of the material was considered and the numerical results were presented [12].

As well-known piezoelectric ceramic transducers are often designed as a hollow cylinder with multilayers. In the present paper, a long piezo-thermoelastic thick-walled hollow cylinder with double layers is analyzed. The effects of temperature on the performance of the cylinder are studied. Based on the theory of elasticity and using the mixed solving method, the exact solutions for the cylinder submitted to some coupled loadings are obtained. In the present investigation, differences in the material parameter g_{31} in different layers are taken

Y. Chen, Z. F. Shi (✉)
School of Civil Engineering, Beijing Jiaotong University, Beijing 100044, P. R. China.
E-mail: chying@126.com; zfshi178@sohu.com

into account. For comparison, numerical results have been carried out for both double-layered and graded cylinders subjected to two different kinds of loadings. At the end of the present paper, some inherent properties and discussions have been addressed.

2 Basic equations for piezo-thermoelastic materials under plane-strain conditions

For a long thick-walled hollow cylinder poled in the radial direction and submitted to a symmetric loading on any cross section, the problem can be considered under plane-strain condition. A polar coordinate system (r, θ) is used in the present analysis. Let ε_{ij}, σ_{ij}, D_i, E_i denote the components of strain, stress, induction and electric field strength of the piezoelectric media, respectively. The constitutive equations of a piezo-thermoelastic material under plane-strain conditions can be expressed in the habitual form as [13]

$$\begin{cases} \varepsilon_\theta = s_{11}\sigma_\theta + s_{13}\sigma_r + g_{31}D_r - \mu_{11}T \\ \varepsilon_r = s_{13}\sigma_\theta + s_{33}\sigma_r + g_{33}D_r - \mu_{33}T \\ \gamma_{r\theta} = s_{44}\tau_{r\theta} + g_{15}D_\theta \end{cases} \qquad \begin{cases} E_\theta = -g_{15}\tau_{r\theta} + \zeta_{11}D_\theta \\ E_r = -g_{31}\sigma_\theta - g_{33}\sigma_r + \zeta_{33}D_r - q_3T \end{cases} \tag{1}$$

where s_{ij}, g_{ij} and ζ_{ij} are the coefficients of the effective elastic compliance, piezoelectric and dielectric impermeability, respectively; T is the temperature rise; μ_{ii} and q_3 are the thermal strain and pyroelectric coefficients of the material, respectively. Without consideration of body force and body charge, the equilibrium equations can be given as

$$\begin{cases} \frac{\partial\sigma_r}{\partial r} + \frac{1}{r}\frac{\partial\tau_{r\theta}}{\partial\theta} + \frac{\sigma_r-\sigma_\theta}{r} = 0 \\ \frac{\partial\tau_{r\theta}}{\partial r} + \frac{1}{r}\frac{\partial\sigma_\theta}{\partial\theta} + \frac{2\tau_{r\theta}}{r} = 0 \end{cases} \qquad \frac{1}{r}\frac{\partial D_\theta}{\partial\theta} + \frac{\partial D_r}{\partial r} + \frac{D_r}{r} = 0 \tag{2}$$

In steady state, the temperature field is governed by Fourier's heat conduction equation

$$\frac{\partial^2 T}{\partial r^2} + \frac{1}{r}\frac{\partial T}{\partial r} + \frac{1}{r^2}\frac{\partial^2 T}{\partial\theta^2} = 0 \tag{3}$$

The components of strain and electric field strength are related to the displacement $(u_\theta,\ u_r)$ and electrical potential ϕ by the following equations

$$\begin{cases} \varepsilon_\theta = \frac{u_r}{r} + \frac{1}{r}\frac{\partial u_\theta}{\partial\theta}, \quad \varepsilon_r = \frac{\partial u_r}{\partial r} \\ \gamma_{r\theta} = \frac{1}{r}\frac{\partial u_r}{\partial\theta} + \frac{\partial u_\theta}{\partial r} - \frac{u_\theta}{r} \end{cases} \qquad \begin{cases} E_\theta = -\frac{1}{r}\frac{\partial\phi}{\partial\theta} \\ E_r = -\frac{\partial\phi}{\partial r} \end{cases} \tag{4}$$

Based on the theory of elasticity, the compatibility equation expressed by the components of strain can be obtained as

$$\left(\frac{\partial^2}{\partial r^2} + \frac{2}{r}\frac{\partial}{\partial r}\right)\varepsilon_\theta + \left(\frac{1}{r^2}\frac{\partial^2}{\partial\theta^2} - \frac{1}{r}\frac{\partial}{\partial r}\right)\varepsilon_r = \left(\frac{1}{r^2}\frac{\partial}{\partial\theta} + \frac{1}{r}\frac{\partial^2}{\partial r\partial\theta}\right)\gamma_{r\theta} \tag{5}$$

In the following sections these basic equations will be used to study the behavior of a double-layered piezo-thermoelastic hollow cylinder.

3 Exact analysis of a double-layered piezo-thermoelastic hollow cylinder

Piezoelectric materials have been widely used to produce sensors and actuators in engineering. Besides, piezoelectric materials (such as piezoelectric ceramics) are also a class of transducer materials [14,15]. As mentioned above, piezoelectric ceramic transducers are often designed as a hollow cylinder with multilayers. In the present paper, an exact analysis of a double-layered piezo-thermoelastic hollow cylinder will be presented and the effects of temperature on the performance of the cylinder will be studied. It should be noted that the dielectric and elastic coefficients depend on the degree of polling. However, as demonstrated by some experimental investigations, this dependence is less pronounced than that of the piezoelectric coefficients g_{31} in *type-g* or d_{31} in *type-d* constitutive equations [16,17]. Therefore, for simplicity, except the piezoelectric coefficient g_{31}, the dielectric and elastic coefficients are assumed to be constant for all the layers in the present investigation. In detail, the piezoelectric parameter g_{31} of the material will be denoted by g_{31i} for layer $i\,(i = 1, 2)$, and the other corresponding parameters of the material as well as the coefficient of thermal conductivity in each layer are assumed to be the same. The thickness of layer i is determined by the inner radius R_i and the outer radius R_{i+1}, as shown in Fig. 1. The temperature rise of layer i at the inner and outer surfaces are denoted by T_{1i} and T_{2i}, respectively.

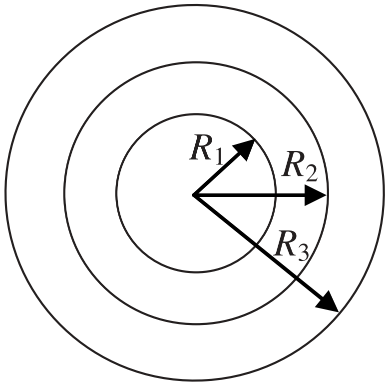

Fig. 1 Cross section of a hollow cylinder with double layers

3.1 Solutions of a piezo-thermoelastic monolayer cylinder

For the piezo-thermoelastic hollow cylinder with double layers shown in Fig. 1 the exact solutions can be found based on the theory of elasticity when the cylinder is subjected symmetrically to some coupled thermal and mechanical as well as electric loadings. First the general solution of a random monolayer is studied. To find the mechanical field of the piezo-thermoelastic hollow cylinder, the Airy stress function method is used. The stress function and the electric potential of layer i are denoted by φ_i and ϕ_i, respectively. For symmetry, the components of stress and electric field strength can be expressed as

$$\sigma_{\theta i} = \varphi_i''(r), \quad \sigma_{ri} = \frac{1}{r}\varphi_i'(r), \quad \tau_{r\theta i} = 0 \tag{6}$$

$$E_{\theta i} = 0, \quad E_{ri} = -\phi_i'(r) \tag{7}$$

By using Eq. (1), we obtain

$$D_{\theta i} = 0, \quad \gamma_{r\theta i} = 0 \tag{8}$$

It is easily found from Eq. (3) that the temperature field is related to the temperature change only. Therefore, the temperature field can be solved first. Supposing that the piezoelectric hollow cylinder is homogeneously heated at the surface, the temperature rise of the inner and outer surfaces of each sub-cylinder remains constant at T_{1i} and T_{2i}, respectively. This means we have the following thermal boundary conditions

$$T_i(r = R_i) = T_{1i}\ , \quad T_i(r = R_{i+1}) = T_{2i} \tag{9}$$

By symmetry, the heat conduction equation (3) can be simplified to

$$T_i''(r) + \frac{1}{r}T_i'(r) = 0 \tag{10}$$

The solution of above equation can be found as

$$T_i(r) = t_{1i}\ln r + t_{0i} \tag{11}$$

where

$$t_{0i} = \frac{T_{1i}\ln R_{i+1} - T_{2i}\ln R_i}{\ln R_{i+1} - \ln R_i}, \quad t_{1i} = \frac{T_{2i} - T_{1i}}{\ln R_{i+1} - \ln R_i} \tag{12}$$

Having obtained the distribution of temperature field, we will try to find the mechanical and electrical fields. Substituting Eqs. (6) and (7) into Eq. (2), yields

$$\frac{\mathrm{d}D_{ri}}{\mathrm{d}r} + \frac{D_{ri}}{r} = 0 \tag{13}$$

The general solution of this equation is

$$D_{ri} = \frac{a_{0i}}{r} \tag{14}$$

where a_{0i} is an unknown constant to be determined. Keeping Eq. (1) in mind, the compatibility equation (5) can be rewritten as

$$s_{11}\varphi_i^{(4)}(r)r^3 + 2s_{11}\varphi_i'''(r)r^2 - s_{33}\varphi_i''(r)r + s_{33}\varphi_i'(r) + (\mu_{33} - \mu_{11})t_{1i}r + g_{33}a_{0i} = 0 \tag{15}$$

After integrating, the above equation becomes

$$\varphi_i'(r) = a_{1i}r + b_i r\ln r + c_{1i}r^s + c_{2i}r^{-s} + c_i \tag{16}$$

where

$$s = \sqrt{\frac{s_{33}}{s_{11}}}, \quad b_i = \frac{t_{1i}(\mu_{33} - \mu_{11})}{s_{33} - s_{11}}, \quad c_i = -\frac{g_{33}}{s_{33}}a_{0i} \tag{17}$$

in which a_{1i}, c_{1i} and c_{2i} are unknown constants to be determined. Substituting Eq. (16) into Eq. (6), the stress components can be expressed as

$$\begin{cases} \sigma_{\theta i} = a_{1i} + b_i\ln r + b_i + c_{1i}sr^{s-1} - c_{2i}sr^{-s-1} \\ \sigma_{ri} = a_{1i} + b_i\ln r + c_{1i}r^{s-1} + c_{2i}r^{-s-1} + c_i r^{-1} \\ \tau_{r\theta i} = 0 \end{cases} \tag{18}$$

The strain components can be found from Eq. $(1)_1$ as

$$\begin{cases} \varepsilon_{\theta i} = (s_{11}s + s_{13})c_{1i}r^{s-1} - (s_{11}s - s_{13})c_{2i}r^{-s-1} + (s_{13}c_i + g_{31i}a_{0i})r^{-1} \\ \qquad +[(s_{11} + s_{13})b_i - \mu_{11}t_{1i}]\ln r + [(s_{11} + s_{13})a_{1i} + s_{11}b_i - \mu_{11}t_{0i}] \\ \varepsilon_{ri} = (s_{13}s + s_{33})c_{1i}r^{s-1} - (s_{13}s - s_{33})c_{2i}r^{-s-1} \\ \qquad +[(s_{13} + s_{33})b_i - \mu_{33}t_{1i}]\ln r + [(s_{13} + s_{33})a_{1i} + s_{13}b_i - \mu_{33}t_{0i}] \\ \gamma_{r\theta i} = 0 \end{cases} \tag{19}$$

Further, the displacement components can be obtained by the use of Eq. (4) as

$$\begin{cases} u_{ri} = \frac{s_{13}s + s_{33}}{s}c_{1i}r^s + \frac{s_{13}s - s_{33}}{s}c_{2i}r^{-s} + (s_{13}c_i + g_{31i}a_{0i}) \\ \qquad +[(s_{13} + s_{33})b_i - \mu_{33}t_{1i}](\ln\ r - 1)r + [(s_{13} + s_{33})a_{1i} + s_{13}b_i - \mu_{33}t_{0i}]r + A_{1i}\sin\ \theta + A_{2i}\cos\ \theta \\ u_{\theta i} = A_{1i}\cos\ \theta - A_{2i}\sin\ \theta + B_i r \end{cases} \tag{20}$$

where A_{1i}, A_{2i} and B_i are unknown constants. Taking the condition of single-valued displacement into account, we obtain

$$a_{1i} = \frac{(s_{33} + s_{11})b_i + (\mu_{33} - \mu_{11})t_{0i} - \mu_{33}t_{1i}}{s_{33} - s_{11}} \tag{21}$$

On the other hand, to find the electric potential, Eq. $(1)_2$ is expressed as

$$\begin{cases} E_{\theta i} = 0 \\ E_{ri} = -(g_{31i}s + g_{33})c_{1i}r^{s-1} + (g_{31i}s - g_{33})c_{2i}r^{-s-1} - (g_{33} - \varsigma_{33}a_{0i})r^{-1} \\ \qquad -[(g_{31i} + g_{33})b_i + q_3t_{1i}]\ln r - (g_{31i} + g_{33})a_{1i} - g_{31i}b_i - q_3t_{0i} \end{cases} \tag{22}$$

By the use of Eq. (4), the electric potential can be obtained as follows:

$$\begin{aligned} \phi_i = {} & \frac{g_{31i}s + g_{33}}{s}c_{1i}r^s + \frac{g_{31i}s - g_{33}}{s}c_{2i}r^{-s} + (g_{33}c_i - \varsigma_{33}a_{0i})\ln r \\ & +[(g_{31i} + g_{33})b_i + q_3t_{1i}](\ln r - 1)r + [(g_{31i} + g_{33})a_{1i} + g_{31i}b_i + q_3t_{0i}]r + F_i \end{aligned} \tag{23}$$

where F_i is another unknown constant.

It is obvious that once the unknown parameters a_{0i}, c_i, c_{1i}, c_{2i}, A_{1i}, A_{2i}, B_i and F_i are determined by using some suitable boundary conditions, the distributions of all the mechanical and electrical components such as the stress, electric field strength and displacement as well as electric potential in each layer can be found.

3.2 Exact solutions of a double-layered hollow cylinder under different loadings

Now let us try to assemble the above solution to find the solutions of a double-layered hollow cylinder under different loadings. Without loss of generality it is assumed that the double layers (with the same coefficient of thermal conductivity k) are in complete contact at the interface. First the continuity conditions at the interface ($r = R_2$) can be considered as follows:

$$T_{12} = T_{21}, \quad k\frac{\partial T_1}{\partial r} = k\frac{\partial T_2}{\partial r} \tag{24_1a}$$

$$\sigma_{r1} = \sigma_{r2}, \quad \tau_{r\theta 1} = \tau_{r\theta 2}, \quad u_{r1} = u_{r2}, \quad u_{\theta 1} = u_{\theta 2} \tag{24_1b}$$

$$D_{r1} = D_{r2}, \quad \phi_1 = \phi_2 \tag{24_1c}$$

These connecting conditions result in

$$\begin{cases} t_{01} = t_{02} = t_0, \quad t_{11} = t_{12} = t_1 \\ b_1 = b_2 = b = \frac{t_1(\mu_{11} - \mu_{33})}{s_{11} - s_{33}} \\ a_{11} = a_{12} = a_1 = \frac{(s_{11} + s_{33})b + (\mu_{33} - \mu_{11})t_0 - \mu_{33}t_1}{s_{33} - s_{11}} \\ (c_{11} - c_{12})R_2^{s-1} + (c_{21} - c_{22})R_2^{-s-1} = 0 \\ \frac{s_{13}s + s_{33}}{s}(c_{11} - c_{12})R_2^{s} + \frac{s_{13}s - s_{33}}{s}(c_{21} - c_{22})R_2^{-s} + \Delta[g_{31}]_{12}a_0 = 0 \\ A_{11} = A_{12} = A_1, \\ A_{21} = A_{22} = A_2, \\ B_1 = B_2 = B \\ a_{01} = a_{02} = a_0, \\ c_1 = c_2 = c \\ F_1 - F_2 = \sum_{i=1}^{2}\sum_{j=1}^{2}(-1)^i \frac{g_{31i}s - (-1)^j g_{33}}{s} c_{ji} R_2^{-(-1)^j s} - \Delta[g_{31}]_{12}(a_1 + b\ln R_2)R_2 \end{cases} \tag{25}$$

where the symbols t_0, t_1, b, a_0, a_1 and c are introduced, and $\Delta[g_{31}]_{12} = g_{311} - g_{312}$. To determine the unknown constants, the piezo-thermoelastic hollow cylinder subjected to three kinds of coupled loadings will be studied separately.

Case I—Subjected to a thermal loading only

In this case, the temperature rise at the inner and outer surfaces of the cylinder is assumed to be T_1 and T_2 respectively. So the parameters t_0 and t_1 can be obtained from Eqs. (9), (11) and (25) as:

$$\begin{cases} t_1 = \frac{T_2 - T_1}{\ln R_3 - \ln R_1} \\ t_0 = \frac{T_1 \ln R_3 - T_2 \ln R_1}{\ln R_3 - \ln R_1} \end{cases} \tag{26}$$

Thus the distribution of temperature field can be determined by Eq. (11). On the other hand, let us consider the following electrical and mechanical boundary conditions.

$$\begin{cases} D_{r1}(r = R_1) = D_{r2}(r = R_3) = 0 \\ \phi_1(r = R_1) = 0 \end{cases}, \quad \begin{cases} \sigma_{r1}(r = R_1) = \sigma_{r2}(r = R_3) = 0 \\ \tau_{r\theta 1}(r = R_1) = \tau_{r\theta 2}(r = R_3) = 0 \end{cases} \tag{27}$$

With the aid of Eq. (25), all the unknown constants relating the stress and electric fields can be given as

$$\begin{cases} a_0 = 0, \quad c_1 = c_2 = c = 0 \\ c_{11} = c_{12} = \hat{c}_1 = \frac{\hat{N}_1}{\hat{N}}, \quad c_{21} = c_{22} = \hat{c}_2 = \frac{\hat{N}_2}{\hat{N}} \\ F_1 = -\sum_{j=1}^{2} \frac{g_{311}s - (-1)^j g_{33}}{s}\hat{c}_j R_1^{-(-1)^j s} - [(g_{311} + g_{33})b + q_3 t_1](\ln R_1 - 1)R_1 \\ \qquad -[(g_{311} + g_{33})a_1 + g_{311}b + q_3 t_0]R_1 \\ F_2 = -\sum_{i=1}^{2}\sum_{j=1}^{2} \frac{g_{31i}s - (-1)^j g_{33}}{s}\hat{c}_j \Delta[R^{-(-1)^i s}]_{(i)(4-2i)} + \Delta[g_{31}]_{12}(a_1 + b\ln R_2)R_2 \\ \qquad -[(g_{311} + g_{33})b + q_3 t_1](\ln R_1 - 1)R_1 - [(g_{311} + g_{33})a_1 + g_{311}b + q_3 t_0]R_1 \end{cases} \tag{28}$$

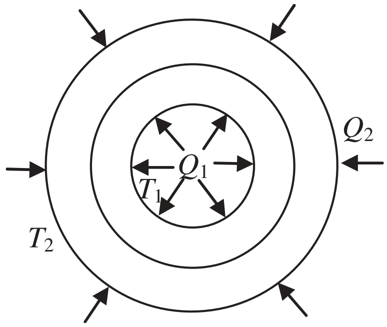

Fig. 2 The cylinder subjected to thermal and mechanical loadings

in which

$$\hat{N} = \begin{vmatrix} R_1^{s-1} & R_1^{-s-1} \\ R_3^{s-1} & R_3^{-s-1} \end{vmatrix}, \quad \hat{N}_1 = \begin{vmatrix} -a_1 - b\ln R_1 & R_1^{-s-1} \\ -a_1 - b\ln R_3 & R_3^{-s-1} \end{vmatrix}, \quad \hat{N}_2 = \begin{vmatrix} R_1^{s-1} & -a_1 - b\ln R_1 \\ R_3^{s-1} & -a_1 - b\ln R_3 \end{vmatrix} \tag{29}$$

Here and in the following we introduce the notations $\Delta[f(R)]_{ij} = f(R_i) - f(R_j)$ and let $R_0 = 0$, $R_4 = R_1$, such as $\Delta[g_{31}]_{ij} = g_{31i} - g_{31j}$, $\Delta[R^{-(-1)^j s}]_{(i)(4-2i)} = R_i^{-(-1)^j s} - R_{4-2i}^{-(-1)^j s}$.

Case II—Subjected to thermal and mechanical loading

For the case of a piezo-thermoelastic cylinder subjected to a thermal and mechanical loading simultaneously, as shown in Fig. 2, the uniform pressures on the inner and outer surfaces will be denoted by Q_1 and Q_2, respectively. The temperature field in this case is the same as in case I. The electric boundary conditions expressed by Eq. $(27)_1$ are also valid. Besides, the mechanical boundary conditions can be expressed by

$$\begin{cases} \sigma_{r1}(r = R_1) = -Q_1 \\ \sigma_{r2}(r = R_3) = -Q_2 \\ \tau_{r\theta 1}(r = R_1) = \tau_{r\theta 2}(r = R_3) = 0 \end{cases} \tag{30}$$

Keeping Eq. (25) in mind, all the unknown constants can be determined as follows:

$$\begin{cases} a_0 = 0, c_1 = c_2 = c = 0 \\ c_{11} = c_{12} = \hat{c}_1 = \frac{\hat{J}_1}{\hat{N}}, \quad c_{21} = c_{22} = \hat{c}_2 = \frac{\hat{J}_2}{\hat{N}} \\ F_1 = -\sum\limits_{j=1}^{2} \frac{g_{311}s-(-1)^j g_{33}}{s} \hat{c}_j R_1^{-(-1)^j s} - [(g_{311} + g_{33})b + q_3 t_1](\ln R_1 - 1)R_1 \\ \qquad -[(g_{311} + g_{33})a_1 + g_{311}b + q_3 t_0]R_1 \\ F_2 = -\sum\limits_{i=1}^{2}\sum\limits_{j=1}^{2} \frac{g_{31i}s-(-1)^j g_{33}}{s} \hat{c}_j \Delta[R^{-(-1)^i s}]_{(i)(4-2i)} + \Delta[g_{31}]_{12}(a_1 + b\ln R_2)R_2 \\ \qquad -[(g_{311} + g_{33})b + q_3 t_1](\ln R_1 - 1)R_1 - [(g_{311} + g_{33})a_1 + g_{311}b + q_3 t_0]R_1 \end{cases} \tag{31}$$

where

$$\hat{J}_1 = \begin{vmatrix} -(Q_1 + b\ln R_1 + a_1) & R_1^{-s-1} \\ -(Q_2 + b\ln R_3 + a_1) & R_3^{-s-1} \end{vmatrix}, \quad \hat{J}_2 = \begin{vmatrix} R_1^{s-1} & -(Q_1 + b\ln R_1 + a_1) \\ R_3^{s-1} & -(Q_2 + b\ln R_3 + a_1) \end{vmatrix} \tag{32}$$

Case III—Subjected to thermal and electric loading

For the case of a piezo-thermoelastic cylinder subjected to a thermal and electric loading simultaneously, as shown in Fig. 3, the solution of temperature field is the same as in case I. The electric boundary conditions can be expressed as follows:

$$\begin{cases} \phi_2(r = R_3) = V_0 \\ \phi_1(r = R_1) = 0 \end{cases} \tag{33}$$

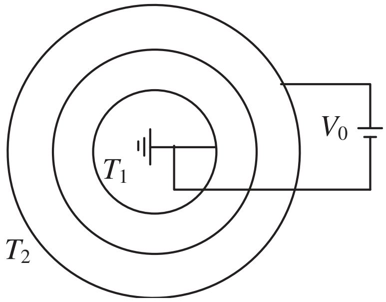

Fig. 3 The cylinder subjected to thermal and electric loadings

The mechanical boundary conditions are the same as Eq. $(27)_2$. By the use of Eq. (25), all the unknown constants can be determined as follows:

$$\begin{cases} a_0 = \frac{s_{33}(V_0+\hat{\xi})}{g_{33}\xi}, c_1 = c_2 = c = -\frac{V_0+\hat{\xi}}{\xi}, c_{ji} = \xi_{ji}c + \hat{\xi}_{ji} \quad (i, j = 1, 2) \\ F_1 = -\sum\limits_{j=1}^{2} \frac{g_{311}s-(-1)^j g_{33}}{s} c_{j1} R_1^{-(-1)^j s} - (g_{33} + \frac{\varsigma_{33}s_{33}}{g_{33}})c \ln R_1 \\ \qquad -[(g_{311}+g_{33})b + q_3 t_1](\ln R_1 - 1)R_1 - [(g_{311}+g_{33})a_1 + g_{311}b + q_3 t_0]R_1 \\ F_2 = -\sum\limits_{i=1}^{2}\sum\limits_{j=1}^{2} \frac{g_{31i}s-(-1)^j g_{33}}{s} c_{ji} \Delta[R^{-(-1)^j s}]_{(i)(4-2i)} - (g_{33} + \frac{\varsigma_{33}s_{33}}{g_{33}})c \ln R_1 \\ \qquad -[(g_{311}+g_{33})b + q_3 t_1](\ln R_1 - 1)R_1 - [(g_{311}+g_{33})a_1 + g_{311}b + q_3 t_0]R_1 \\ \qquad +\Delta[g_{31}]_{12}(a_1 + b \ln R_2)R_2 \end{cases} \tag{34}$$

where the following denotations are introduced:

$$\begin{aligned} & b_1 = b_2 = 0, \quad b_3 = b, \quad g_{313} = -g_{33}, \quad q_1 = q_2 = 0 \\ \xi_{ji} &= \sum_{i=1}^{2}\sum_{j-1}^{2} \left\{ \frac{(-1)^j - 1}{2} R_{(2i-1)}^{-s} - \frac{[R_{(2i-1)}^{-2s}]^{2-j}}{\Delta[R^{-2s}]_{23}} \left[\Delta[R^{-s}]_{13} - \frac{(-1)^j \Delta g_{31}}{2g_{33}} s R_2^s \Delta[R^{-2s}]_{(3-i)(4-i)} \right] \right\} \\ \hat{\xi}_{ji} &= \sum_{i=1}^{2}\sum_{j-1}^{2} \left\{ \frac{(-1)^j - 1}{2} [a_1 + b \ln R_{(2i-1)}] R_{(2i-1)}^{-s+1} - \frac{[R_{(2i-1)}^{-2s}]^{2-j}}{\Delta[R^{-2s}]_{23}} \Delta[(a_1 + b \ln R)R]_{13} \right\} \\ \xi &= \sum_{i=1}^{2}\sum_{j-1}^{2} \frac{g_{31i}s - (-1)^j g_{33}}{s} \xi_{ji} \Delta[R^{-(-1)^j s}]_{(i+1)(i+2)} + g_{33}\Delta[\ln R]_{13}] \\ \hat{\xi} &= \sum_{i=1}^{2}\sum_{j-1}^{2} \frac{g_{31i}s - (-1)^j g_{33}}{s} \hat{\xi}_{ji} \Delta[R^{-(-1)^j s}]_{i(i+1)} + \sum_{i=1}^{3} (b g_{31i} - q_i t_1)\Delta[(\ln R - 1)R]_{i(i+1)} \\ & + \sum_{i=1}^{3} [(a_1 + b - b_i)g_{31i} - q_i t_0]\Delta[R]_{i(i+1)} \end{aligned} \tag{35}$$

The unknown constants for a double-layered thick-walled hollow cylinder subjected to some coupled loadings have now been determined. Given these constants, all the distributions of stress, strain, displacement and electric potential of the hollow cylinder can be found by the use of Eqs. (18), (19), (20) and (23), respectively.

4 Numerical results and discussions

To give a clear explanation, numerical results are reported in this section. A cylinder made of cadmium selenide will be considered and both layers of the cylinder are assumed to have the same thickness. The radius of the inner and outer surfaces of the cylinder is taken to be 10 and 20 mm, respectively. The piezoelectric parameter g_{31} of the inner and outer layers is taken to be -41.66×10^{-3} m^2/C and -70.00×10^{-3} m^2/C, respectively. The other material parameters of the cylinder are listed in Table 1.

Table 1 Some material parameters of cadmium selenide [18]

Elastic constant ($\times 10^{-12}$ m^2/N)				Piezoelectric constant ($\times 10^{-3}$ m^2/C)		Dielectric impermeability constant ($\times 10^9$ m/F)		Thermal strain constant ($\times 10^{-7}$ 1/K)		Pyroelectric coefficient ($\times 10^3$) N/(K·C)
s_{11}	s_{13}	s_{33}	s_{44}	g_{33}	g_{15}	ζ_{11}	ζ_{33}	μ_{11}	μ_{33}	q_3
23.20	−5.38	16.68	74.62	83.25	−12.48	11.91	10.62	−42.50	−27.49	−37.10

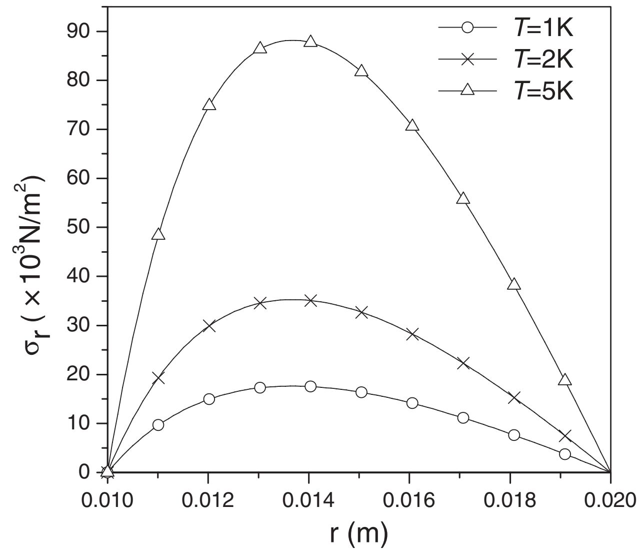

Fig. 4 Distribution of the normal stress σ_r

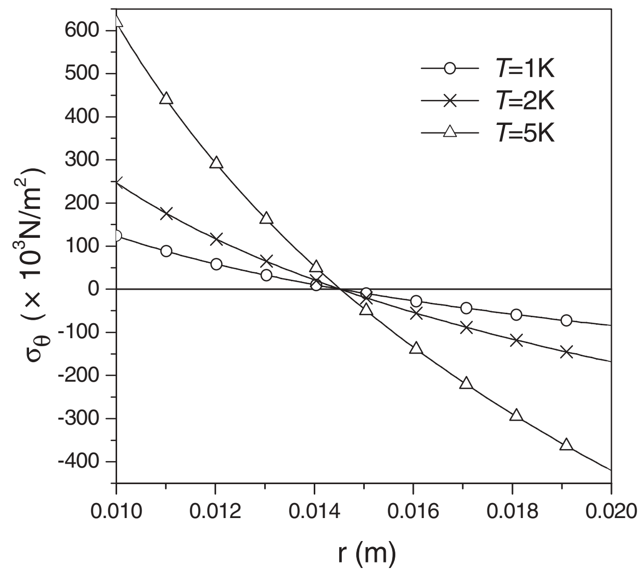

Fig. 5 Distribution of the normal stress σ_θ

For the cylinder subjected to temperature rise only, the distributions of normal stresses σ_r, σ_θ and the relative displacement Δu_r as well as the electric potential $\Delta\phi$ are plotted in Figs. 4–7, respectively. It is easily found that, with increasing temperature rise, the output of the mentioned components will increase. The effect of the temperature rise on the electric potential output in the double-layered cylinder is consistent with that found in the investigations on the piezo-thermoelastic plate and shell [9, 18].

On the other hand, some analytical methods and theoretical solutions of functionally graded piezoelectric cantilevers were presented in our previous works [19–23]. To make a comparison, a piezo-thermoelastic hollow

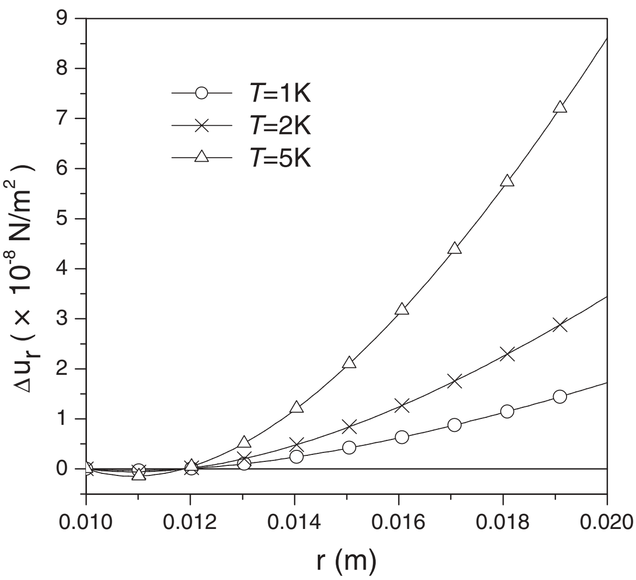

Fig. 6 The relative displacement Δu_r

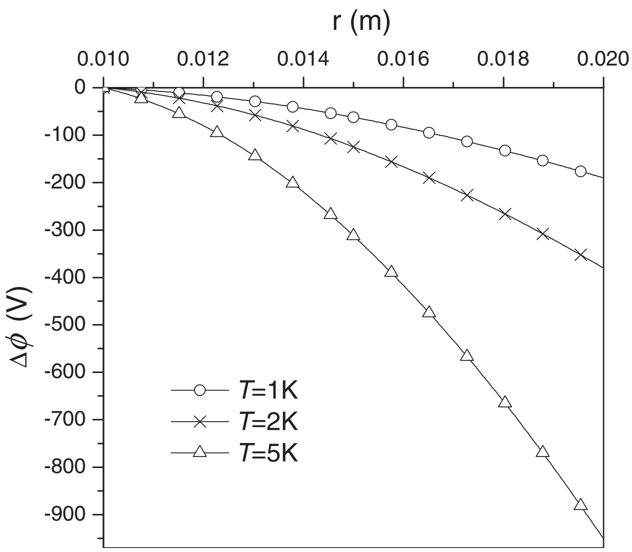

Fig. 7 Distribution of the electric potential $\Delta\phi$

cylinder with a linearly graded parameter g_{31} is also studied in the present paper. The geometrical size of the graded cylinder is the same as the double-layered cylinder. That is to say that the expression $g_{31} = m_1 r + m_0$ is considered, in which the two coefficients m_i are determined as $m_1 = -28.33 \times 10^{-1}$ and $m_0 = -13.33 \times 10^{-3}$ so that g_{31} has the value -41.66×10^{-3} m^2/C and -70.00×10^{-3} m^2/C at the inner and outer surfaces, respectively. The other material parameters of the cylinder are the same as given in Table 1. By the use of the same method as used in Sect. 3, the exact solutions for the cylinder submitted to thermal loading and some coupled loadings have been obtained, such as

$$\sigma_\theta = \hat{a} + \hat{b}\ln r + \hat{b} + \hat{c}_1 s r^{s-1} - \hat{c}_2 s r^{-s-1}, \sigma_r = \hat{a} + \hat{b}\ln r + \hat{c}_1 r^{s-1} + \hat{c}_2 r^{-s-1} + \hat{c} r^{-1} \quad (36)$$

where $\hat{a}$, $\hat{b}$, $\hat{c}_1$, $\hat{c}_2$ and $\hat{c}$ are constants to be determined by using boundary conditions. When the FGM cylinder is subjected to an electric potential V_0 between the inner and outer surfaces only, these unknown constants can be found as

$$\hat{a} = \frac{1}{s_{33} - s_{11}} \frac{H_3}{H} m_1, \quad \hat{c}_1 = \frac{H_1}{H}, \quad \hat{c}_2 = \frac{H_2}{H}, \quad \hat{c} = -\frac{g_{33}}{s_{33}} \frac{H_3}{H}, \quad \hat{b} = 0 \tag{37}$$

in which

$$\begin{aligned}
H_1 &= V_0 \begin{vmatrix} R_1^{-s-1} & Y_1 \\ R_2^{-s-1} & Y_2 \end{vmatrix}, \quad H_2 = -V_0 \begin{vmatrix} R_1^{s-1} & Y_1 \\ R_2^{s-1} & Y_2 \end{vmatrix}, \quad H_3 = V_0 \begin{vmatrix} R_1^{s-1} & R_1^{-s-1} \\ R_2^{s-1} & R_2^{-s-1} \end{vmatrix}, \\
H &= \begin{vmatrix} R_1^{s-1} & R_1^{-s-1} & Y_1 \\ R_2^{s-1} & R_2^{-s-1} & Y_2 \\ W_1 & W_2 & W_3 \end{vmatrix}, \quad Y_i = \frac{m_1}{s_{33} - s_{11}} - \frac{g_{33}}{s_{33}} R_i^{-1} (i = 1, 2), \\
W_1 &= \sum_{i=0}^{1} \frac{m_i s + d_i}{s + i} \Delta[R^{s+i}]_{21}, \quad W_2 = -\sum_{i=0}^{1} \frac{m_i s - d_i}{-s + i} \Delta[R^{-s+i}]_{21}, \\
W_3 &= \sum_{i=0}^{1} \frac{1}{i+1} \frac{m_1}{s_{33} - s_{11}} (m_i + d_i) \Delta[R^{i+1}]_{21} + \left(\frac{g_{33}^2}{s_{33}} - \varsigma_{33} \right) \Delta[\ln R]_{21},
\end{aligned} \tag{38}$$

where

$$d_0 = g_{33}, d_1 = 0$$

Figure 8 shows the difference between the electric potential in the double-layered cylinder and in the graded cylinder under the same temperature rise of $T = 1\,\mathrm{K}$. For both cylinders subjected to an electric potential $V_0 = 100\,\mathrm{V}$, the distributions of normal stresses σ_r and σ_θ are plotted in Fig. 9 and 10, respectively. These figures show that the internal stresses are drastically reduced in materials and devices with functionally graded properties.

5 Conclusions

Based on the theory of elasticity, the present analysis provides some exact solutions for a double-layered piezo-thermoelastic hollow cylinder under some coupled loadings. It is found that, with an increasing temperature rise, the amplitudes of the mechanical and electric components of the cylinder will increase, and the internal stresses can be drastically reduced in functionally graded materials and structures.

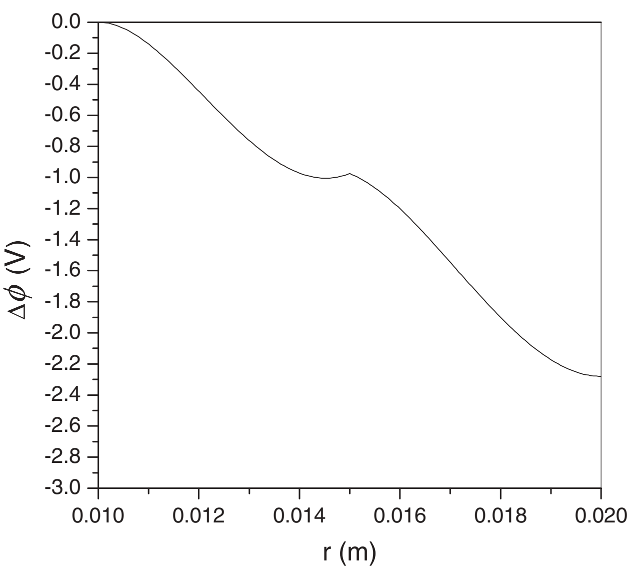

Fig. 8 Difference of the electric potential between the two models: $\Delta\phi = \phi_{\mathrm{FGM}} - \phi_{\mathrm{bimorph}}$ at $T = 1\,\mathrm{K}$

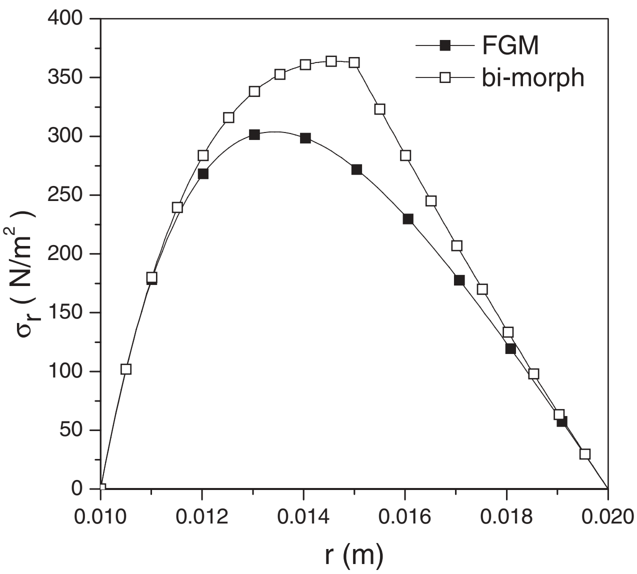

Fig. 9 The normal stress σ_r of the cylinder in the different analytical models at $V = 100\,\mathrm{V}$

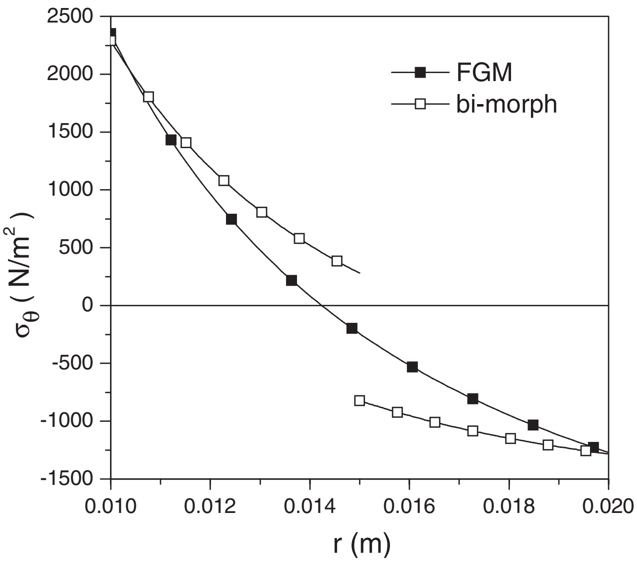

Fig. 10 The normal stress σ_θ of the cylinder in the different analytical models at $V = 100\,\mathrm{V}$

Acknowledgements This work is supported by the National Natural Science Foundation of China (50272003) and by the Teaching and Research Award Fund for Outstanding Young Teachers in Higher Education Institutions of MOE, P.R.C.

References

1. Olesiak, Z.S., Pyryev, Y.U.A.: A coupled quasi-stationary problem of thermodiffusion for an elastic cylinder. Int J Eng Sci **33**, 773–780 (1995)
2. Ting, T.C.T.: New solutions to pressuring, shearing, torsion and extension of a circular tube or bar. Proc R Soc Lond A **455**, 3527–3542 (1999)
3. Chen, T.Y., Chung, C.T., Lin, W.L.: A revisit of a cylindrically anisotropic tube subjected to pressuring, shearing, torsion, extension, and a uniform change. Int J Solids Struct **37**, 5143–5159 (2000)
4. Ding, H.J., Wang, H.M., Chen, W.Q.: Analytical solution for the electroelastic dynamics of a nonhomogeneous spherically isotropic piezoelectric hollow sphere. Arch Appl Mech **73**, 49–62 (2003)
5. Hou, P.F., Wang, H.M., Ding, H.J.: Analytical solution for the axisymmetric plane strain electroelastic dynamics of a special non-homogeneous piezoelectric hollow cylinder. Int J Eng Sci **41**, 1849–1868 (2003)

6. Sharma, J.N., Pal, M., Chand, D.: Three-dimensional vibration analysis of a piezothermoelastic cylindrical panel. Int J Eng Sci **42**, 1655–1673 (2004)
7. Ootao, Y., Tanigawa, Y.: Control of transient thermoelastic displacement of a two-layered composite plate constructed of isotropic elastic and piezoelectric layers due to nonuniform heating. Arch Appl Mech **71**, 207–220 (2001)
8. Shabana, Y.M., Noda, N.: Thermo-elasto-plastic stresses in functionally graded materials under consideration of the fabrication process. Arch Appl Mech **71**, 649–660 (2001)
9. Ashida, F., Tauchert, T.R.: A general plane-stress solution in cylindrical coordinates for a piezothermoelastic plate. Int J Solids Struct **38**, 4969–4985 (2001)
10. Qin, Q.H., Mai, Y.W.: Thermoelectroelastic Green's function and its application for bimaterial of piezoelectric materials. Arch Appl Mech **68**, 433–444 (1998)
11. Birman, V.: Thermal effects on measurements of dynamic processes in composite structures using piezoelectric sensors. Smart Mater Struct **5**, 379–385 (1996)
12. Tian, X.G, Shen, Y.P.: Finite element analysis of thermo-mechanical behaviour of piezoelectric structures under finite deformation. Acta Mech Solida Sin **24**, 169–178 (2003)
13. Wu, X.H, Shen, Y.P, Chen, C.Q.: An exact solution for functionally graded piezothermoelastic cylindrical shell as sensors or actuators. Mater Lett **57**, 3532–3542 (2003)
14. McMahon, G.W.: The ring-shell flextensional transducer (class v). In: Hamonic, B.F., Wilson, O.B., Decarpigny, J.N. (Eds.) Power transducers for sonics and ultrasonics, Springer, Berlin Heidelberg New York, pp. 60–74, (1991)
15. Berlincourt, D.: Piezoelectric crystals and ceramics in ultrasonic transducer materials. In: Mattiat, O.E. (Ed.) Plenum, New York (1971)
16. Kouvatov, A., Steinhausen, R., Seifert, W., Hauke, T., Langhammer, H.T., Beige, H., Abiche, H.: Comparison between bimorphic and polymorphic bending devices. J Eur Ceram Soc **3**, 1153–1156 (2001)
17. Hauke, T., Kouvatov, A., Steinhausen, R., Seifert, W., Beige, H., Langhammer, H.T., Abicht, H.: Bending behavior of functionally gradient materials. Ferroelectrics **238**, 195–202 (2000)
18. Kapuria, S., Dumir, P.C., Sengupta, S.: Exact piezothermoelastic axisymmetric solution of a finite transversely isotropic cylindrical shell. Comput Struct **61**(6), 1085–1099 (1996)
19. Shi, Z.F.: General solution of a density functionally gradient piezoelectric cantilever and its applications. Smart Mater Struct **11**, 122–129 (2002)
20. Shi, Z.F.; Chen Y.: Functionally graded piezoelectric cantilever under load. Arch Appl Mech **74**, 237–247 (2004)
21. Liu, T.T., Shi, Z.F.: Bending behavior of functionally gradient piezoelectric cantilever. Ferroelectrics. **308**, 43–51 (2004)
22. Chen, Y., Shi, Z.F.: Exact solutions of functionally gradient piezo-thermal-elastic cantilevers and parameter identification. J Intell Mat Syst Struct **16**(6), 531–539 (2005)
23. Shi, Z.F.: Bending behavior of piezoelectric curved actuator. Smart Mater Struct **14**, 835–842 (2005)